MAXIMUM A POSTERIORI SUPER-RESOLUTION OF COMPRESSED VIDEO WITH A NOVEL MULTICHANNEL IMAGE PRIOR AND A NEW OBSERVATION MODEL

Stefanos P. Belekos[1,3]*, Nikolaos P. Galatsanos*[2]*, and Aggelos K. Katsaggelos*[1,3]

[1] Faculty of Physics, University of Athens/Senior Network Engineer at Vodafone-GR,
[2] Department of Electrical and Computer Engineering, University of Patras,
[3] Department of Electrical Engineering and Computer Science, Northwestern University,
Evanston, IL, 60208-3118, USA, stefbel@phys.uoa.gr, aggk@eecs.northwestern.edu

ABSTRACT

In this paper we propose a class of SR algorithms for compressed video using the maximum *a posteriori* (MAP) approach. These algorithms utilize a novel multichannel image prior model which has already been presented mainly for uncompressed video, along with a new hierarchical Gaussian nonstationary version of the state-of-the-art quantization noise model. The relationship between model components and the decoded bitstream is also demonstrated. An additional novelty of this framework pertains to the transition flexibility from totally nonstationary algorithms used for compressed video to fully stationary algorithms used for raw video. Numerical simulations comparing the proposed models among themselves, verify the efficacy of the adopted multichannel nonstationary prior for different compression ratios, and the significant role of the nonstationary observation term.

1. INTRODUCTION

Improving the resolution of a frame or a set of frames belonging in a video sequence, by utilizing the non redundant information provided by a sequence of LR decoded frames. The *super-resolution (SR)* problem impacts a wide variety of signal processing applications. For example, SR aims at enhancing the precision of scientific, medical, and space imaging systems, improves the robustness of tracking tasks, and benefits consumer electronic and entertainment applications such as, cell phones, digital video cameras, portable Digital Versatile Discs (DVD), and High Definition Televisions (HDTV) [1]. In each of these systems, acquiring data using a high resolution system increases significantly system complexity. Consequently, SR algorithmic techniques become really important for achieving this goal. Moreover, while many techniques have been proposed to enhance uncompressed video (see for example [1]- [4]), only a few have been introduced to efficiently improve the resolution of compressed video (e.g., [5], [6]) There is also a significant gap on proposing a unified class of SR algorithms for both compressed and uncompressed data. On the other hand, the use of an algorithm designed for raw data but applied to decompressed data, discards important information about the quantization noise that was introduced in the HR frames during compression.

In this paper we address the compressed video SR problem within the context of the MAP framework. The main novelties of this work are mainly two. The first one, stems from the fact that it extends the utilization of the recently proposed *nonstationary* multichannel prior from uncompressed [3] to compressed video, given that its stationary version has already been adopted for decoded video sequences [5]. Moreover, it is the first time that the single frame counterpart of the nonstationary prior [3] is also used for compressed video. The second novelty is the introduction of two *new nonstationary hierarchical observation models* for the decoded frames by utilizing the same assumptions stated in [3] for the prior, in the observation terms (quantization noise) proposed in [5]. Consequently, a class of new video SR algorithms results with the transition flexibility from fully nonstationary algorithms for compressed data to fully stationary algorithms for raw video by selecting only four parameters.

This paper is organized as follows. In Sec.2 we present the mathematical background. In Sec. 3 we introduce a general MAP problem formulation for the SR of compressed video resulting in three new algorithms and their asymptotic cases. Numerical experiments are provided in Sec. 4, indicating the superiority of the nonstationary prior for different bit-rates and the contribution of the new observation models in certain cases. Finally, Sec. 5 concludes the paper.

2. MATHEMATICAL BACKGROUND

2.1. Observation Models

As clearly stated in [5] and [6], compression noise is attributed to quantization noise and also the motion vectors (MVs) which are provided in the compressed bit-stream. Following the steps in [5], [6], we also use two different observation models related to quantization noise. However, the *novel factor adopted* in this paper, is the fact that we formulate their nonstationary (hierarchical two-level Gaussian) versions in total allignment with the respective methodology proposed in [3], for the prior model. More specifically, by treating the *spatially varying precisions per pixel* (related to quan-

tization and registration noise) as Random Variables (RVs) described by a Gamma hyperprior, we capture in a more realistic way their heavy-tailed (Student-t like) nature, especially in the cases of high compression rates.

Following the analysis in [5] and [6] the first proposed imaging model, which describes the quantization noise, is given by

$$\mathbf{y}_i = \mathbf{DHf}_i + \mathbf{e}_i, \tag{1}$$

where $\mathbf{D}$ is the $MN \times LMLN$ down-sampling matrix, $\mathbf{H}$ is the $LMLN \times LMLN$ known blurring matrix, $\mathbf{y}_i$ is the compressed observation of the ith LR frame, $\mathbf{f}_i$ is its HR counterpart (of dimensions $MN \times 1$ and $LMLN \times 1$, respectively) and $\mathbf{e}_i \sim N(\mathbf{0}, \mathbf{U}_i)$ with $\mathbf{U}_i$ being the covariance matrix in the spatial domain. Moreover, given that this is the *stationary* version of the aforementioned model (assuming an IID noise process, or equivalently AWGN) $\mathbf{U}_i = \zeta_i^{-1}\mathbf{I}$, where $\mathbf{I}$ is the identity matrix of size $MN \times MN$ and ζ_i is the inverse quantization noise variance (precision parameter).

Based on the framework proposed in [3], we introduce the *nonstationary* form of the aforementioned observation model which comprises a novelty of this work. Therefore, we define the spatially varying quantization noise error *per pixel* as $e_{i,\nu} \sim N(0, (\upsilon_{i,\nu})^{-1})$ (ν=1,..,MN), along with the vectors-matrices $\boldsymbol{\upsilon}_i = [\upsilon_{i,1}, \upsilon_{i,2}, \ldots, \upsilon_{i,MN}]^T$, $\boldsymbol{\upsilon}^{total} = [\boldsymbol{\upsilon}_{k-m}^T, \ldots, \boldsymbol{\upsilon}_k^T, \ldots, \boldsymbol{\upsilon}_{k+m}^T]^T$ and $\mathbf{U}_i^{-1} = \text{diag}\{\upsilon_{i,1}, \upsilon_{i,2}, \ldots, \upsilon_{i,MN}\}$, where $i = k-m, \ldots, k, \ldots, k+m$. Moreover, assuming *statistical independency* for the quantization errors, the following improper Gauss pdf occurs (non-AWGN assumption)

$$p(\mathbf{y}_i|\mathbf{f}_i, \boldsymbol{\upsilon}_i) \propto \prod_{\nu=1}^{MN} (\upsilon_{i,\nu})^{1/2} \exp\left(-\frac{1}{2}((\mathbf{y}_i - \mathbf{DHf}_i)^T \mathbf{U}_i^{-1}(\mathbf{y}_i - \mathbf{DHf}_i))\right). \tag{2}$$

Assuming a Gamma hyperprior for the RVs $\upsilon_{i,\nu}$ i.e.,

$$p(\upsilon_{i,\nu}; \lambda_i, \psi_i) \propto (\upsilon_{i,\nu})^{\frac{\psi_i - 2}{2}} \exp(-\lambda_i(\psi_i - 2)\upsilon_{i,\nu}), \tag{3}$$

along with their statistical independency

$$p(\boldsymbol{\upsilon}_i; \lambda_i, \psi_i) = \prod_{\nu=1}^{MN} p(\upsilon_{i,\nu}; \lambda_i, \psi_i), \tag{4}$$

we obtain the proposed two-level hierarchical (Student-t) like form of the quantization error.

Utilizing exactly the same references and arguments for the second imaging model proposed in [5], its stationary version is defined as

$$\mathbf{y}_i = \mathbf{DHM}_{i,k}\mathbf{f}_k + \mathbf{e}_{i,k}, \tag{5}$$

where $\mathbf{M}(\mathbf{d}_{i,k}) = \mathbf{M}_{i,k}$ is the 2-D motion compensation matrix of size $LMLN \times LMLN$ and $\mathbf{e}_{i,k} \sim N(\mathbf{0}, \mathbf{U}_{i,k})$ is the quantization noise model with $\mathbf{U}_{i,k}$ representing the covariance matrix in the spatial domain for the ith frame, where $\zeta_{i,k}$ is the precision related to both quantization and registration noise components ($\mathbf{U}_{i,k} = \zeta_{ik}^{-1}\mathbf{I}$).

To formulate the respective *novel nonstationary* version of this model we use the following definitions (in total alignment with the previous observation models): $e_{ik,\nu} \sim N(0, (\upsilon_{ik,\nu})^{-1}$, $\boldsymbol{\upsilon}_{ik} = [\upsilon_{ik,1}, \upsilon_{ik,2}, \ldots, \upsilon_{ik,MN}]^T$, $\boldsymbol{\upsilon}_{i,k}^{total} = [\boldsymbol{\upsilon}_{k-m,k}^T, \ldots, \boldsymbol{\upsilon}_{k,k}^T, \ldots, \boldsymbol{\upsilon}_{k+m,k}^T]^T$ and $\mathbf{U}_{ik}^{-1} = \text{diag}\{\upsilon_{ik,1}, \upsilon_{ik,2}, \ldots, \upsilon_{ik,MN}\}$. Moreover, the respective hierarchical form of the noise term is based on the following equations

$$p(\mathbf{y}_i|\mathbf{f}_k, \boldsymbol{\upsilon}_{ik}) \propto \prod_{\nu=1}^{MN} (\upsilon_{ik,\nu})^{1/2} \exp\left(-\frac{1}{2}((\mathbf{y}_i - \mathbf{DHM}_{ik}\mathbf{f}_k)^T \mathbf{U}_{ik}^{-1}(\mathbf{y}_i - \mathbf{DHM}_{ik}\mathbf{f}_k))\right), \tag{6}$$

$$p(\upsilon_{ik,\nu}; \lambda_{ik}, \psi_{ik}) \propto (\upsilon_{ik,\nu})^{\frac{\psi_{ik} - 2}{2}} \exp(-\lambda_{ik}(\psi_{ik} - 2)\upsilon_{ik,\nu}), \tag{7}$$

$$p(\boldsymbol{\upsilon}_{ik}; \lambda_{ik}, \psi_{ik}) = \prod_{\nu=1}^{MN} p(\upsilon_{ik,\nu}; \lambda_{ik}, \psi_{ik}). \tag{8}$$

The transition of the aforementioned observation models from their nonstationary to the stationary forms takes place in the asymptotic cases where $\psi_i \to \infty$ and $\psi_{ik} \to \infty$, respectively.

Finally, as clearly stated in [5] and [6], in both the aforementioned observation models the noise component by the motion vectors provided in the compressed bitstream should be incorporated, which is efficiently formulated as IID (AWGN) stationary noise process

$$\mathbf{y}_i^{MV} = \mathbf{C}(\mathbf{v}_{i,j})\mathbf{y}_j = \mathbf{DHM}_{i,j}\mathbf{f}_j + \mathbf{w}_{ij,MV}, \tag{9}$$

where given the assumptions stated in those references $\mathbf{w}_{ij,MV} \sim N(\mathbf{0}, \mathbf{R}_{ij,MV})$ and $\mathbf{R}_{ij,MV} = r_{i,j}^{-1}\mathbf{I}$ is the respective covariance matrix in the spatial domain for the ith frame ($r_{i,j}$ is the precision related to the displaced frame difference (DFD)). Obviously, in the case of the second observation model j=k. As is shown in Sec. 3, setting these precision parameters equal to zero, results in the utilization of the presented algorithms for uncompressed data.

2.2. Image Prior Models

In this work we consider two nonstationary prior models (along with their stationary counterparts / *asymptotic cases*) in order to penalize compression errors. The first one, is the novel *nonstationary multichannel* prior proposed in [3] for uncompressed data (the stationary version of it, $l_j^d \to \infty$ and $\xi_{ij} \to \infty$, was used in [3], [4] for raw data and in [5] for compressed video). Moreover, the second one is also referred as single (within) channel nonstationary prior in [3] (its stationary form was also used in [4] and [5] and consists of the well-known single channel prior which is modelled by a SAR distribution). Therefore, the full mathematical background of the utilized priors, along with their qualitative analysis is given in the aforementioned publications and is not repeated in this work, due to space constraints.

3. MAP PROBLEM FORMULATION AND PROPOSED ALGORITHM

In this section we introduce a MAP problem formulation for the SR of compressed video, resulting in three novel non-stationary algorithms. Moreover, their asymptotic (semi-stationary and stationary) versions are mentioned, which occur when only the observation model or both the prior and the observation models are stationary, respectively.

3.1. Algorithm 1

The simplest approach to the studied problem is to use a single decoded channel described by the nonstationary observation model of (1)-(4). In this case no motion information is used and SR takes place without using any of the adjacent channels. Combining these equations with the single (within) channel nonstationary prior in [3] the MAP estimate results in the following novel non-stationary algorithm

$$\alpha_{i,\mu}^{d} = \frac{(\frac{1}{4} + \frac{1}{2}(l_i^d - 2))}{(\frac{1}{2}(\varepsilon_{i,\mu}^{d})^2 + \nu_i^d(l_i^d - 2))}, \tag{10}$$

$$\upsilon_{i,\nu} = \frac{(\frac{1}{2} + \frac{1}{2}(\psi_i - 2))}{(\frac{1}{2}(e_{i,\nu})^2 + \lambda_i(\psi_i - 2))}, \tag{11}$$

$$\left(\mathbf{H}^T\mathbf{D}^T\mathbf{U}_i^{-1}\mathbf{D}\mathbf{H} + \sum_{d=1}^{2}(\mathbf{Q}^d)^T\mathbf{A}_i{}^d\mathbf{Q}^d\right)\hat{\mathbf{f}}_i = \mathbf{H}^T\mathbf{D}^T\mathbf{U}_i^{-1}\mathbf{y}_i, \tag{12}$$

where $\mathbf{D}^T$ defines the up-sampling operation.

Based on the previous analysis, the stationary version of Algorithm 1 has already been proposed in [5], while for its semi-stationary (also new algorithm) version (12) becomes

$$\left(\mathbf{H}^T\mathbf{D}^T\mathbf{D}\mathbf{H} + \zeta_i^{-1}\sum_{d=1}^{2}(\mathbf{Q}^d)^T\mathbf{A}_i{}^d\mathbf{Q}^d\right)\hat{\mathbf{f}}_i = \mathbf{H}^T\mathbf{D}^T\mathbf{y}_i, \tag{13}$$

and ζ_i is also given in [5].

3.2. Algorithm 2

The nonstationary version of this algorithm, comprises also a novel approach. More specifically, it utilizes the nonstationary format of the second observation model (5)-(8), along with (9) (for j=k), while the respective nonstationary prior model of Algorithm 1 is also adopted. Therefore, motion information between video frames is utilized only by the observation model. Consequently, the respective MAP estimate yields

$$\upsilon_{ik,\nu} = \frac{(\frac{1}{2} + \frac{1}{2}(\psi_{ik} - 2))}{(\frac{1}{2}(e_{ik,\nu})^2 + \lambda_{ik}(\psi_{ik} - 2))}, \tag{14}$$

$$r_{ik} = \frac{MN}{\left\|\mathbf{y}_i^{MV} - \mathbf{D}\mathbf{H}\mathbf{M}_{i,k}\mathbf{f}_k\right\|^2}, \tag{15}$$

$$(\tilde{\mathbf{J}} + \sum_{d=1}^{2}(\mathbf{Q}^d)^T\mathbf{A}_k^d\mathbf{Q}^d)\hat{\mathbf{f}}_k = \tilde{\mathbf{Z}}, \tag{16}$$

where

$$\tilde{\mathbf{J}} = \sum_{i=k-m}^{k+m}[\mathbf{M}_{k,i}\mathbf{H}^T\mathbf{D}^T\mathbf{U}_{i,k}^{-1}\mathbf{D}\mathbf{H}\mathbf{M}_{i,k} + r_{ik}\mathbf{M}_{k,i}\mathbf{H}^T\mathbf{D}^T\mathbf{D}\mathbf{H}\mathbf{M}_{i,k}], \tag{17}$$

$$\tilde{\mathbf{Z}} = \sum_{i=k-m}^{k+m}[\mathbf{M}_{k,i}\mathbf{H}^T\mathbf{D}^T\mathbf{U}_{i,k}^{-1}\mathbf{y}_i + r_{ik}\mathbf{M}_{k,i}\mathbf{H}^T\mathbf{D}^T\mathbf{C}_{i,k}\mathbf{y}_k] \tag{18}$$

while the estimation of $\alpha_{i,\mu}^d$ is given by (10) for $i = k$ and $\mathbf{C}_{i,k} = \mathbf{C}(\mathbf{v}_{i,k})$. Similarly to Algorithm 1, the stationary version of Algorithm 2 has already been proposed in [5] and [6], and for its semi-stationary (also novel algorithm) format the steps of the previous analysis are followed.

3.3. Proposed Algorithm 3

In the novel proposed nonstationary Algorithm 3, the nonstationary observation term described by (1)-(4) and the bitstream related observation term expressed by (9), are combined with the new *nonstationary multichannel* prior analyzed in [3]. Following [3]- [6], along with the respective notation, (taking into account all possible combinations of the HR motion fields and the compressed LR motion fields) the objective function becomes $J_{MAP}(\tilde{\mathbf{f}}, \boldsymbol{\alpha}^t, \boldsymbol{\beta}^t, \boldsymbol{\upsilon}^t | \tilde{\mathbf{y}}, \tilde{\mathbf{v}}; \boldsymbol{\lambda}^t, \boldsymbol{\psi}^t\boldsymbol{\nu}^t, \boldsymbol{l}^t, \boldsymbol{\tau}^t, \boldsymbol{\xi}^t, \tilde{\boldsymbol{r}})$ where t stands for total, $\tilde{\mathbf{f}} = [\mathbf{f}_{k-m}^T, \ldots, \mathbf{f}_k^T, \ldots, \mathbf{f}_{k+m}^T]^T$, and $\tilde{\mathbf{y}}$ is the column vector containing the decoded observations. Its minimization results in

$$\upsilon_{i,\nu} = \frac{(\frac{1}{2} + \frac{1}{2}(\psi_i - 2))}{(\frac{1}{2}(e_{i,\nu})^2 + \lambda_i(\psi_i - 2))}, \tag{19}$$

$$r_{ij} = \frac{MN}{\left\|\mathbf{y}_i^{MV} - \mathbf{D}\mathbf{H}\mathbf{M}_{i,j}\mathbf{f}_j\right\|^2}, \tag{20}$$

$$(\tilde{\mathbf{G}} + \tilde{\boldsymbol{\Omega}})\hat{\tilde{\mathbf{f}}} = \tilde{\Lambda}\tilde{\mathbf{y}}, \tag{21}$$

where

$\tilde{\mathbf{G}} = diag\{(\Gamma_{k-m} + \Theta_{k-m}), ..., (\Gamma_{k+m} + \Theta_{k+m})\}$

and

$\tilde{\boldsymbol{\Lambda}} = diag\{(\Delta_{k-m} + \Xi_{k-m}), ..., (\Delta_{k+m} + \Xi_{k+m})\}$,

with

$\Gamma_j = \mathbf{H}^T\mathbf{D}^T\mathbf{U}_j^{-1}\mathbf{D}\mathbf{H}$, $\Theta_j = \sum_{i=k-m}^{k+m} r_{ij}\mathbf{M}_{j,i}\mathbf{H}^T\mathbf{D}^T\mathbf{D}\mathbf{H}\mathbf{M}_{i,j}$,

$\Delta_j = \mathbf{H}^T\mathbf{D}^T\mathbf{U}_j^{-1}$, $\Xi_j = \sum_{i=k-m}^{k+m} r_{ij}\mathbf{M}_{j,i}\mathbf{H}^T\mathbf{D}^T\mathbf{C}_{i,j}$ and $\tilde{\boldsymbol{\Omega}}$ is given in [3]. Finally, in a respective way to the previous algorithms, the stationary version of Algorithm 3 is given in [5], while its semi-stationary format is derived based on the previous analysis and is not given explicitly due to space limitations.

In this algorithm the (HR) MF information is also taken into account through the prior, while *simultaneous SR (and restoration) of all the HR frames is taking place* which is not the case in algorithms 1 and 2. Clearly, all proposed algorithms can be used for both compressed (using also the

motion vector information provided by the compressed bitstream) and not compressed data in each of their three states (nonstationary, semi-stationary and stationary). Finally, (12), (13), (16), and (21) can not be solved in closed form, due to the non-circulant nature of the matrices $\mathbf{D}, \mathbf{M}^T$, $\mathbf{M}$, $\mathbf{C}_{i,j}$ ${\mathbf{A}_i}^d$, $\mathbf{B}_{i,j}$, $\mathbf{U}_i^{-1}$ and $\mathbf{U}_{i,k}^{-1}$. Thus, we resorted to a numerical solution using a *conjugate-gradient (CG) algorithm.*

4. EXPERIMENTAL RESULTS

In this section, we assess experimentally the performance of the developed novel MAP SR Algorithms 1, 2 and 3 in their stationary, semi-stationary, and nonstationary forms by comparing among themselves (relative efficacy) for both compressed and raw video data. Moreover, the stationary algorithms have been tested against their state-of-the-art counterparts and exhibited better performance. Consequently, their advanced nonstationary versions, will also do better than the competition. However, this latter comparison is not shown due to space constraints. In all presented results, the influence of the compression ratio on the SR enhancement process is also taken into consideration, utilizing the H.264 / AVC standard. The central 256×256 region/section of five consecutive frames of the sequence "Mobile" (CIF format), at 30 frames per second was selected for the HR original data. While the first frame of the sequence is intra-coded, each other frame is compressed as a P-frame (baseline profile). Moreover, we tested two limiting bit-rates of 1.63 Mbps (quantization parameter equals to 16) and 199 kbps (quantization parameter equals to 23), simulating a "high" and "low" quality coding video process, respectively.

In the "high" quality case the input sequence to the encoder was not blurred at all ($\mathbf{H} = \mathbf{I}$), whereas in the "low" quality case uniform 9×9 blur was adopted as extra degradation mechanism. After blurring, all frames are sub-sampled by a factor of two ($L = 2$). The objective metrics used to quantify the quality of the results, were ISNR, PSNR, and VIF [3]- [6].

The stationary versions of Algorithms 1, 2 and 3 denoted by *Al1*, *Al2* and *pAl* (proposed algorithm) respectively, were initialized as described in [5]. Moreover, these algorithms were utilized for the initialization of their semi-stationary counterparts which in their turn initialized the respective nonstationary algorithms. The prior related hyperparameters were initialized as mentioned in [3], while the observation model oriented ones are given by $\lambda_i = 1/(2\zeta_i)$ ($\lambda_{ik} = 1/(2\zeta_{ik})$). Moreover, the values of parameters l, ξ and ψ which control the degree of nonstationarity are shown in the tables below along with the experimental outcomes in the case of raw data ($r_{ij} = 0$). Additionally, motion estimation was implemented using a 3-level hierarchical block matching algorithm with integer pixel accuracy at each level. During the CG performance, matrices $\mathbf{M}_{i,j}$ were initially estimated and remained fixed (the same holds for the estimated precision parameters). The same procedure was followed for the estimation of matrices $\mathbf{C}_{i,j}$, given the decoded LR observations, in order to optimize $\mathbf{v}_{i,j}$ vector estimates compared to their values obtained from the compressed bitstream. In all models, the adopted convergence criterion for the termination of the CG algorithm was $\left\|\mathbf{f}_k^{new} - \mathbf{f}_k^{old}\right\|^2 / \left\|\mathbf{f}_k^{old}\right\|^2 < 10^{-6}$.

Based on the presented tables several observations are made. The proposed model (nonstationary Algorithm 3 utilizing the nonstationary prior) is robust in terms of ISNR, PSNR and VIF in the cases where it is used for compressed data compared against all other models, while the nonstationary quantization noise term plays a significant role in nonstationary *Al1 and Al2*. Moreover, the efficacy of the unified class of SR Algorithms for compressed data is much greater compared to its respective use for uncompressed data, due to the removal of the artifacts which are introduced by the compression procedure.

Representative video frames of recovered HR intensities, are depicted in Figs. 1 and 2. Clearly, the novel nonstationary prior utilized in *pAl3*, efficiently removes ringing and blocking artifacts, while it simultaneously denoises smooth areas and preserves edges. The numbers are sharper, stripes are also improved, while in the high bit-rate scenario, where nonstationary *pAl* exhibits its best performance, the circles on the ball are better defined and the tip of the train is less jagged given the removal of compression artifacts. Finally, the nonstationary observation terms are proved to have a strong effect only in denoising the smooth parts of the frames.

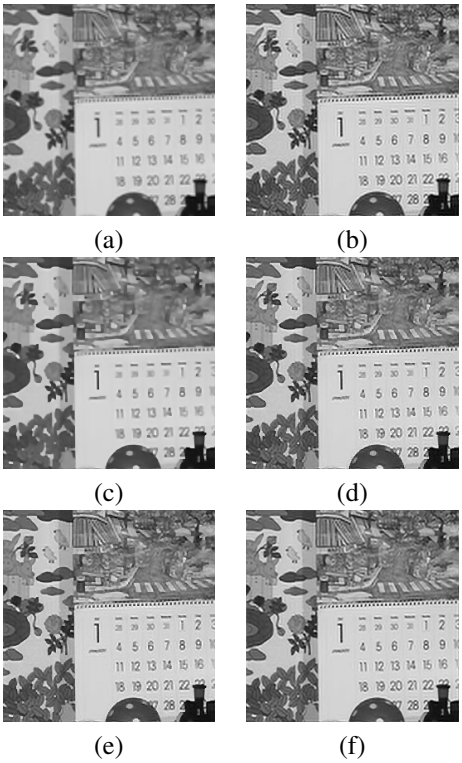

Fig. 1. SR estimates (Bit-Rate: $1.63 Mbps$). Result after (a) bicubic interpol. of the LR observ., (b) stat. *pAl3*, (c) semi-stat. *Al1*, (d) semi-stat. *Al2*, (e) nonstat. *Al2*, (f) nonstat. *pAl3*.

Table 1. Algorithms Using Mobile (Bit-Rate: 1.63Mbps)/Uncompressed Video (No Blur/$\mathbf{H} = \mathbf{I}$)

$1.63Mbps/\mathbf{H} = \mathbf{I}$		ISNR (dB)	PSNR (dB)	VIF	l	ξ	ψ
Stat. Alg.	1	0.69/0.59	20.65	0.26/0.20	–	–	–
	2	2.21/1.89	22.18	0.33/0.28	–	–	–
	3	3.33/2.83	23.30	0.38/0.33	–	–	–
Semi-Stat. Alg.	1	1.89/1.77	21.85	0.34/0.32	2.10	–	–
	2	3.19/2.65	23.16	0.38/0.32	2.10	–	–
	3	4.26/3.58	24.21	0.42/0.37	2.01	5	–
Nonstat. Alg.	1	1.90/1.77	21.86	0.34/0.32	2.10	–	10
	2	3.31/2.66	23.28	0.38/0.32	2.10	–	5
	3	4.28/3.60	24.23	0.42/0.37	2.01	5	10

Table 2. Algorithms Using Mobile (Bit-Rate: 199kbps)/Uncompressed Video (Uniform Blur 9×9)

$199kbps/$Uniform Blur 9×9		ISNR (dB)	PSNR (dB)	VIF	l	ξ	ψ
Stat. Alg.	1	1.27/0.95	18.68	0.16/0.14	–	–	–
	2	1.46/1.23	18.87	0.17/0.16	–	–	–
	3	1.57/1.36	18.98	0.18/0.17	–	–	–
Semi-Stat. Alg.	1	1.55/1.34	18.91	0.18/0.17	2.10	–	–
	2	1.63/1.40	19.04	0.19/0.18	2.10	–	–
	3	1.87/1.66	19.28	0.20/0.19	2.01	5	–
Nonstat. Alg.	1	1.74/1.34	19.10	0.19/0.17	2.10	–	5
	2	1.64/1.40	19.05	0.19/0.18	2.10	–	10
	3	1.89/1.66	19.30	0.20/0.19	2.01	5	8

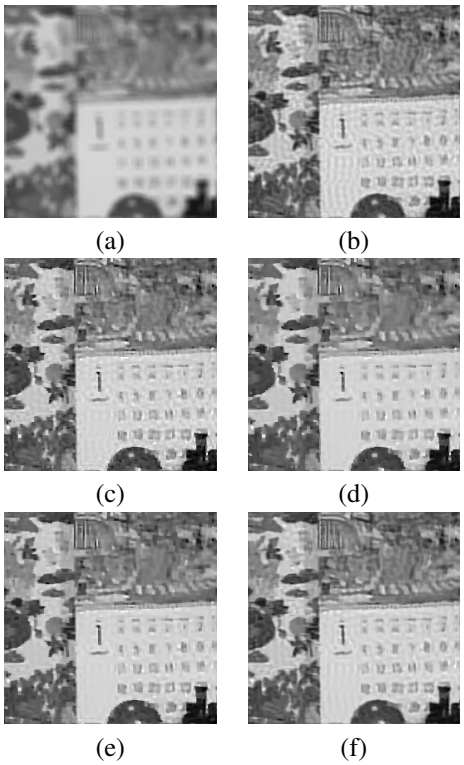

Fig. 2. SR estimates (Bit-Rate: $199kbps$). Result after (a) bicubic interpol. of the LR observ., (b) stat. *pAl3*, (c) semi-stat. *Al1*, (d) semi-stat. *Al2*, (e) nonstat. *Al1*, (f) nonstat. *pAl3*.

5. CONCLUSIONS

In this paper we presented a class of new video SR algorithms, based on the MAP framework, which exhibit the transition flexibility from fully nonstationary algorithms for compressed data to fully stationary algorithms for raw video. Those algorithms exhibited stronger efficacy when used for compressed video compared to raw data. The main contributions of this paper, stem from the utilization of a novel nonstationary prior and of two new nonstationary observation models within the context of compressed video SR. Based on the comparative study of the 3 algorithms, we see that in all experimental cases the proposed algorithm performs better than previous ones in terms of both ISNR and PSNR, as well as VIF. This is a strong indication that the use of MF in the prior term is much more efficient than its use in the observation term, in terms of both restoration capability and resolution enhancement. Finally, as expected, the lower the compression ratio, the more efficient the proposed algorithm is.

6. REFERENCES

[1] A.K. Katsaggelos, R. Molina, and J. Mateos, *Super Resolution of Images and Video*. Morgan & Claypool, 2007.

[2] M.K. Ng, H. Shen, E.Y. Lam, and L. Zhang, "A TV Super-Resolution Reconstruction Algorithm for Digital Video," *EURASIP J. Adv. Signal Proc.*, pp. 1–16, 2007.

[3] S. P. Belekos, N.P. Galatsanos, and A. K. Katsaggelos, "Maximum a posteriori video super-resolution using a new multichannel image prior," *IEEE Trans. Image Proc.*, vol. 19, pp. 1451–1464, Jun. 2010.

[4] S. P. Belekos, N.P. Galatsanos, and A. K. Katsaggelos, "Maximum a posteriori video super-resolution with a new multichannel image prior," in *Proc. EUSIPCO 2008*, Lausanne, Switzerland, Aug. 25-29. 2008, pp. 25–29.

[5] S. P. Belekos, N.P. Galatsanos, S.D. Babacan, and A. K. Katsaggelos, "MAP SR of compressed video using a new multichannel image prior," in *Proc. ICIP 2009*, Cairo, Egypt, Nov. 7-11. 2009, pp. 2797–2800.

[6] C.A. Segall, A. K. Katsaggelos, R. Molina, and J. Mateos, "Bayesian resolution enhancement of compressed video," *IEEE Trans. Image Proc.*, pp. 898–911, Jul. 2004.